

MICROFLUIDIC ENABLED RAPID BIOPRINTING OF HYDROGEL μ FIBER BASED POROUS CONSTRUCTS

Minghao Nie¹, Pritesh Mistry², Jing Yang² and Shoji Takeuchi¹

¹Institute of Industrial Science, University of Tokyo, Tokyo, JAPAN

²School of Pharmacy, University of Nottingham, Nottingham, UK

ABSTRACT

A rapid and high-resolution bioprinter based on a capillary coaxial microfluidic printer head and vacuum substrate, was conceived and built up in this work. We demonstrate the printing of porous (400 μ m pitch) 3D bio-scaffolds made from calcium alginate microfibers with a printing resolution (i.e. fiber diameter) of ca. 150 microns, at a speed of 40 mm/s, which is approximately 10x faster than existing systems with comparable resolution.

INTRODUCTION

Background

Historically, MEMS ink-jet heads have boosted the revolution in traditional printing industry [1]. Recently, with the rapid progress in 3D-printing research and development, new opportunities for the application of MEMS/microfluidic printheads have emerged [2–4]. Specifically, for the field of bioprinting (i.e. the 3D-printing using biomaterials), microfluidic-based printheads have drawn increasing attention; the ability of MEMS/microfluidic printheads to precisely eject extremely small amounts of sample has drastically increased the printing resolution; for example, using co-axial microfluidic nozzles, the resolution of bioprinting has been improved to ~ 100 μ m [5], [6]. In addition, with apt design, one could also switch between different bio-inks on-the-fly using MEMS/microfluidic-based printheads [6], [7]. However, previous systems either

cannot print porous constructs [5], [7], or lack in printing speed (~ 4 mm/s [6]). Porosity is key for sufficient nutrient delivery in densely packed cellular constructs, and printing speed directly affects the throughput, an important factor from an industrial point of view. In this work, we prototyped a bioprinter which is capable of rapidly printing porous 3D constructs made of biomaterial (specifically, alginate, in this work).

Concept of this work

To build up the rapid bioprinter with high printing resolution, two components were important: the printhead (as well as the liquid injection scheme) and the substrate. In this work, we adopted a capillary-based co-axial microfluidic device (with injection via syringe pumps) as the printhead, and a membrane filter-like structure as the substrate.

Compared to the previously reported PDMS-based microfluidic printhead [5], the capillary co-axial microfluidic device is able to form a more stable hydrodynamic focusing of the co-axial fluids due to its uniquely confined three-dimensional geometry configuration. In addition, the long thin shape of glass capillary tubes is similar to a dispensing needle, which is favorable for precise liquid thread dispensing. The solidification of alginate was achieved by introducing sodium alginate in the core channel and a crosslinking agent (calcium chloride) in the sheath channel, as shown

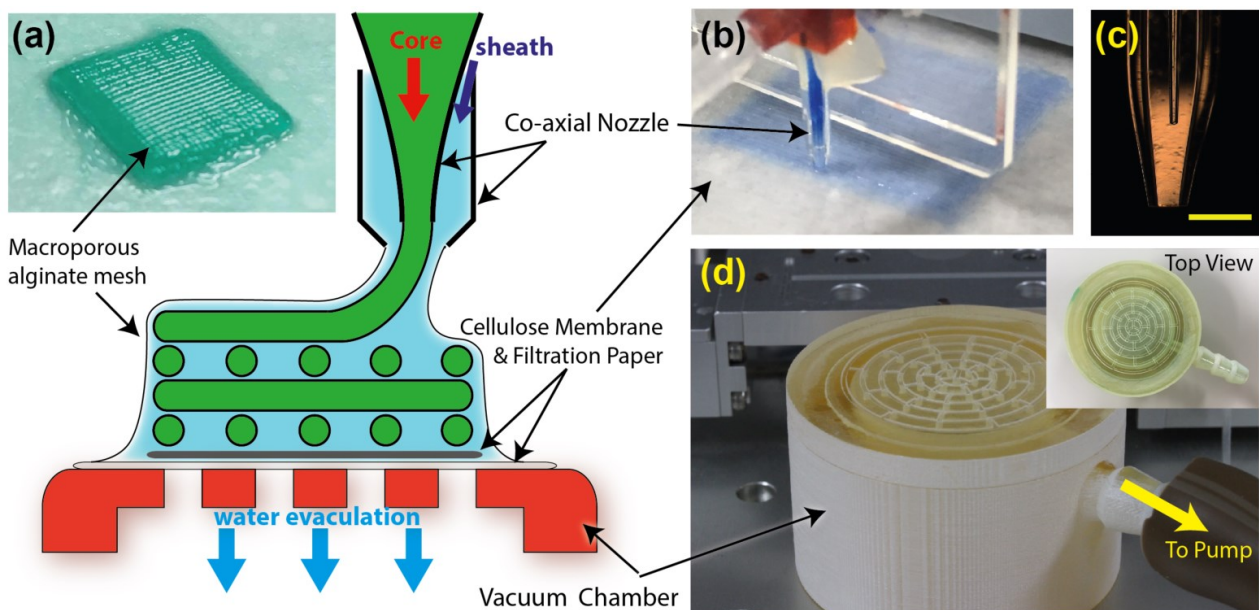


Figure 1: Concept description. (a) Schematic of the microfluidic-based bioprinting system, inset: image of printed construct; (b) the co-axial microfluidic printer head; (c) microscopic image of the printhead tip, scale bar: 500 μ m; (d) the customized vacuum chamber, inset: top view.

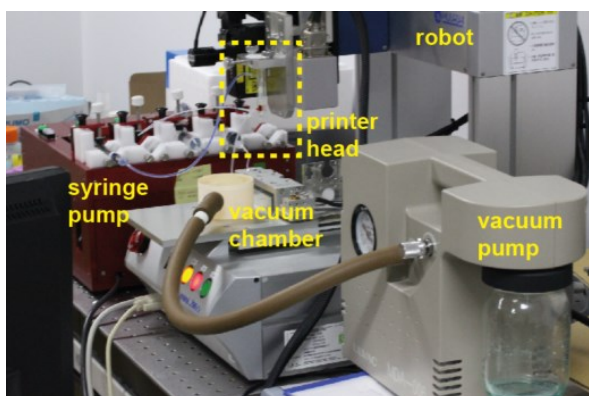


Figure 2: The overall setup including the syringe pump, dispensing robot and vacuum pump.

schematically in Fig. 1(a).

In order to ramp up the printing speed, the dispensing flowrates had to be increased accordingly. Such increases in dispensing flowrates may cause problems in which the remnant crosslinking solution (calcium chloride in this work) pool on the substrate; the pooled fluid will disrupt the surface rheology during printing, and subsequently cause the dispensed alginate fibers to float/misalign. To solve this problem, we designed a substrate by mimicking membrane filter systems that have been used intensely in

chemical laboratories. The substrate consisted of a vacuum chamber and two layers of filter membrane. The membrane was mechanically supported on top of the vacuum chamber, with pneumatic holes connecting the membrane to the vacuum. Once wetted, the filter membranes would not permit air to pass through unless a very strong vacuum was applied (i.e. water breakthrough pressure). The mesh geometry design of the pneumatic holes was optimized to prevent the membrane from warping when the vacuum was applied.

MATERIALS & METHODS

In detail, the microfluidic printer head was made by assembling tapered glass capillaries (round/square capillaries for core/sheath channels, respectively) using a customized fluid connector (Fig. 1b). Distance from the tip of the inner capillary to the tip of outer capillary was ca. 600 μm (Fig. 1c). The tip was rendered hydrophobic using Sigmacote prior to printing. Hydrophobicity eased the transport of liquids to the substrate, whilst the needle-like tip, with a thin capillary wall (<150 μm), helped to increase the jetting speed of bio-inks, which was key to raising the printing speed. The printhead was clamped onto the head of a dispensing robot, and all microfluidic inlets were connected to a 5-axis syringe pump (Fig. 2).

In addition to the printhead, a customized vacuum chamber was fabricated using a commercial 3D printer (Fig. 1d). A two-layer filter, onto which the fibers were

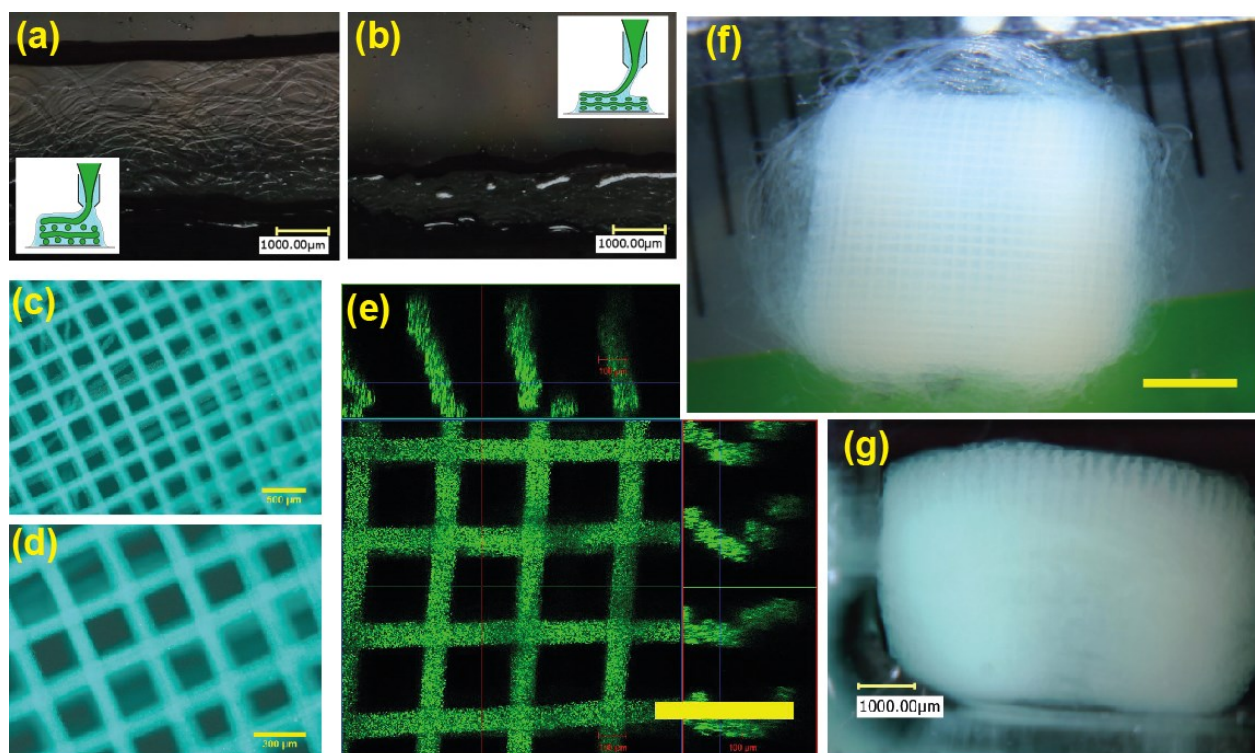


Figure 3: Experimental results. (a) without vacuum, the deposited structure tends to float in the pool of sheath fluids, resulting in bad alignment; (b) with a constant strong vacuum, the alginate fibers were compressed onto the substrate, also resulting in decreased printing quality. (c, d) microscopic image from the top; (e) orthogonal image acquired by confocal microscopy; (f) DSLR image of the printed construct, top view. (g) DSLR image of the printed image, side view; the height is approximately 4.5 mm. Scale bars: (c) 500 μm , (d) 300 μm , (e) 500 μm , (f) 2.5 mm, (g) 1 mm.

printed, was set on top of the vacuum chamber. The chamber design prevented the warping of substrate under vacuum, as the membrane was supported by the structure beneath. The top and bottom layers of the filter were cellulose membrane (2 μm pore size) and filtration paper, respectively. Each served to limit the water evacuation rate and to mechanically strengthen the filter.

For the printing process, sodium alginate (2 wt%, loaded with fluorescent beads and green inks) and calcium chloride (40 mM) were chosen as core and sheath fluids with flowrates of 15 and 200 $\mu\text{L}/\text{min}$, respectively. The robot moved at a speed of 40 mm/s. At the beginning of the printing, the vacuum was set to a high level, which facilitated the neat patterning of alginate fibers, at the expense of flattening the initial 5-6 layers deposited. These “raft layers” were sacrificial and facilitated the printing of the final construct. After the raft layers were printed, the vacuum was set to a low level, and maintained until the end of the printing process. The control of the vacuum was achieved by manually tuning the butterfly valve inside the vacuum pump.

RESULTS & DISCUSSION

We first evaluated the impact of no vacuum versus constant vacuum on the printed fibers. Without vacuum, the deposited structure tended to float in the pool of sheath fluid, resulting in bad alignment; with constant strong vacuum, the alginate fibers were compressed onto the substrate, resulting in decreased printing quality. Relative results are shown in Fig. 3(a, b).

Detailed characterization of the printed construct was as follows. First, the printed constructs were inspected using digital cameras and fluorescent microscopy (Fig. 3). The printed fiber diameter was $\sim 150\ \mu\text{m}$ with 400 μm pitch, as shown in Fig. 3(c, d). To investigate the three-dimensional structure, confocal microscopy was performed with the orthogonal photo taken as shown in Fig. 3(e). The deposited fibers still showed a certain extent of misalignment and flattening. The misalignments were expected as the dispensing robot used had a moving substrate, which caused constant vibration of the printed constructs during the printing process. The flattening of the fibers may indicate that a milder vacuum and more rapid gelation of alginate (which could be achieved by increasing the calcium concentration of crosslinking solution) are necessary in further optimization in the future. To verify that the printed structures are self-supportable, a construct consisting of 144 layers of meshed alginate fibers was printed with a height of ca. 4.5 mm (Fig. 3g).

SUMMARY

In this work, a rapid and high-resolution bioprinter based on a capillary coaxial microfluidic printhead and vacuum substrate was built and tested. We demonstrated the printing of porous (400 μm pitch) 3D bio-scaffolds made up of calcium alginate microfibers with a printing resolution (i.e. fiber diameter) of ca. 150 microns, at a speed of 40 mm/s, which is approximated 10x faster than the existing systems with comparable resolution. We believe that using the platform proposed in this work,

high quality printing of cell-laden alginate porous 3D structures could be printed in a rapid manner. Our techniques are also anticipated to print core/shell type alginate jacketed cell-laden fibers, since our printhead has potential to be extended to multiple axis co-axial printhead; such capability might broaden the application of microfiber-based bottom-up tissue engineering.

ACKNOWLEDGEMENTS

This work was partially supported by Grant-in-Aid for Scientific Research (S) (Grant number: 16H06329).

REFERENCES

- [1] M. J. Madou, *Fundamentals of microfabrication: the science of miniaturization*. CRC press, 2002.
- [2] C. Colosi, M. Costantini, R. Latini, S. Ciccarelli, A. Stampella, A. Barbeta, M. Massimi, L. C. Devirgiliis, and M. Dentini, “Rapid prototyping of chitosan-coated alginate scaffolds through the use of a 3D fiber deposition technique,” *Journal of Materials Chemistry B*, vol. 2, no. 39, pp. 6779–6791, 2014.
- [3] S. Ghorbanian, M. A. Qasaimeh, M. Akbari, A. Tamayol, and D. Juncker, “Microfluidic direct writer with integrated declogging mechanism for fabricating cell-laden hydrogel constructs,” *Biomedical microdevices*, vol. 16, no. 3, pp. 387–395, 2014.
- [4] J. O. Hardin, T. J. Ober, A. D. Valentine, and J. A. Lewis, “Microfluidic printheads for multimaterial 3d printing of viscoelastic inks,” *Advanced Materials*, vol. 27, no. 21, pp. 3279–3284, 2015.
- [5] S. Beyer, A. Bsoul, A. Ahmadi, and K. Walus, “3D alginate constructs for tissue engineering printed using a coaxial flow focusing microfluidic device,” in *2013 Transducers & Eurosensors XXVII: The 17th International Conference on Solid-State Sensors, Actuators and Microsystems (TRANSDUCERS & EUROSENSORS XXVII)*, 2013, pp. 1206–1209.
- [6] C. Colosi, S. R. Shin, V. Manoharan, S. Massa, M. Costantini, A. Barbeta, M. R. Dokmeci, M. Dentini, and A. Khademhosseini, “Microfluidic Bioprinting of Heterogeneous 3D Tissue Constructs Using Low-Viscosity Bioink,” *Advanced Materials*, vol. 28, no. 4, pp. 677–684, 2016.
- [7] S. Beyer, T. Mohamed, and K. Walus, “A Microfluidics Based 3D Bioprinter with On-The-Fly Multimaterial Switching capability,” in *17th International Conference on Miniaturized Systems for Chemistry and Life Sciences*, 2013.

CONTACT

*M.H. Nie, tel: +81-3-54526650; nie@iis.u-tokyo.ac.jp